Exploring the chiral phase transition of $N_f = 2$ flavour QCD with valence overlap fermions

E.-M. Ilgenfritz
ilgenfri@physik.hu-berlin.de

QCD in extreme conditions, Frascati, August 7, 2007

In collaboration with:

V. Weinberg, K. Koller, Y. Koma, Y. Nakamura,
G. Schierholz, T. Streuer

&

– DIK Collaboration –

The DIK (DESY-ITEP-Kanazawa) Collaboration :

DESY:
Y. Nakamura, G. Schierholz, V. Weinberg
associated E.-M. I. (HU Berlin)

ITEP:
V. Bornyakov, S. Morozov, E. Lushchevskaya, M. Polikarpov

Kanazawa:
T. Suzuki, T. Sekido, M. Hasegawa, K. Ishiguro
associated Y. Koma (Numazu College of Technology)

Outline

1. Introduction
   - Motivation
   - Simulation parameters
   - Critical temperature and string tensions around T_c
2. Properties of the lowest eigenmodes
   - Distribution and density of the eigenmodes
   - Localisation of the eigenmodes
   - Local chirality of the eigenmodes
3. Distribution of the topological charge
4. The UV-filtered field strength tensor and its local (anti-)selfduality
5. Summary

Motivation

Nature and order of the QCD finite temperature transition still not well understood and subject of recent research ($\rightarrow$ LAT07 talks by Karsch/Fodor).

- Goal:
  - Insight into the changes of the topological and (anti-)selfdual structure of the gauge fields in the vicinity of the phase transition,
  - understanding of the interplay of the chiral properties / localisation of low-lying fermionic modes and chiral symmetry breaking,
  - microscopic understanding of the chiral symmetry breaking/restoration aspects of the finite temp. transition.
- Overlap fermions are an appropriate tool to investigate the nature of the phase transition from first principles:
  - exact chiral symmetry on the lattice,
  - non/zero modes with global chirality $0/\pm 1$,
  - clear realisation of the index theorem on the lattice.
- Truncated spectral decomposition using the eigenmodes of the Dirac operator acts as an UV-filter and allows ,,nondestructive inspection“.
- Application of tools developed in the context of our research of the structure of the QCD vacuum at $T = 0$ (arXiv:0705.0018 [hep-lat]).

Simulation parameters

$24^3 \times 10,\ \beta = 5.20$

κ	# confs	# $Q = 0$ confs	T/T_c	$1/a$ [MeV]
0.1348	131	8	0.91	1802
0.1352	86	12	0.97	1909
0.1353	131	21	0.98	1936
0.1354	97	11	1.00	1964
0.1355	118	18	1.01	1993
0.1358	122	38	1.06	2080
0.1360	97	40	1.09	2140

$T_c = 197(2)$MeV, $\kappa_c = 0.13542(6)$ (via Polyakov loop method)
PoS(LAT2005)157 (talk then given by Y. Nakamura)

The action

Gauge action: Wilson action

Hybrid approach for fermions:

sea quarks: $N_f = 2$ flavours of clover-improved Wilson fermions

improved sea quark action

$$S_F = S_F^{(0)} - \frac{i}{2}\, \kappa\, g\, c_{SW}\, a^5 \sum_s \bar{\psi}(s)\, \sigma_{\mu\nu}\, F_{\mu\nu}(s)\, \psi(s)$$

mass range: $1.3 < r_0 m_\pi < 2.9$

$r_0 m_\pi$ and r_0/a obtained by interpolation/extrapolation of results by QCDSF/UKQCD

Simulation parameters

×	$16^3 \times 8$,	$\beta = 5.2/5.25$	← PRD 71,114504(2005), PoS(LAT2005)171
• (blue)	$24^3 \times 10$,	$\beta = 5.20$	← PoS(LAT2005)157, this talk (also V. Weinberg at LAT07)
• (red)	$24^3 \times 12$,	$\beta = 5.29$	← Bornyakov's LAT07 talk, overlap analysis started

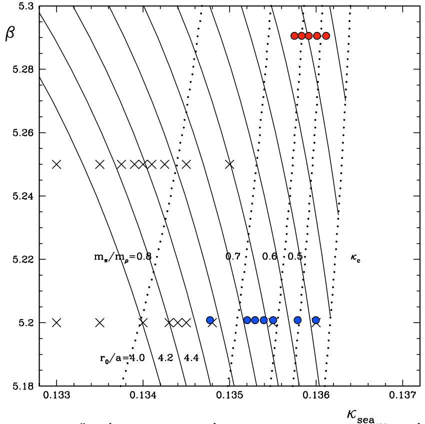

$$T = 1/\left(N_t a(\beta, \kappa_{\rm sea})\right)$$

Lines of constant $\frac{r_0}{a}$ (solid lines) and constant $\frac{m_\pi}{m_\rho}$ (dotted lines) at $T = 0$.

Hybrid approach:

sea quarks: $N_f = 2$ flavours of clover-improved Wilson fermions

valence quarks: overlap fermions (50 eigenmodes computed)

The massive overlap operator

$$D(m_q) = (1 - \frac{am_q}{2\rho})\, D(0) + m_q,$$

$$D(0) = \frac{\rho}{a}(1 + \frac{D_W}{\sqrt{D_W^\dagger D_W}}), D_W = M - \frac{\rho}{a},$$

The improved overlap operator

$$D^{\mathrm{imp}}(0) = \left(1 - \frac{a}{2\,\rho}\; D(0)\right)^{-1} D(0)\;.$$

$$D^{\mathrm{imp}}(m_q) = D^{\mathrm{imp}}(0) + m_q\;.$$

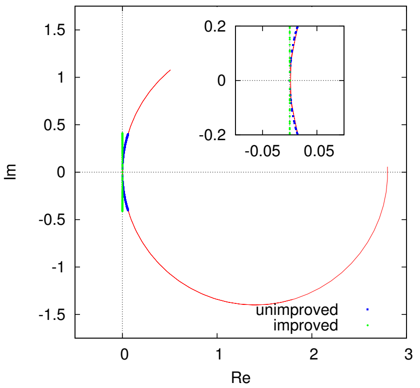

Critical temperature

V. Bornyakov at LAT07 (New data from $N_\tau = 12$ available)

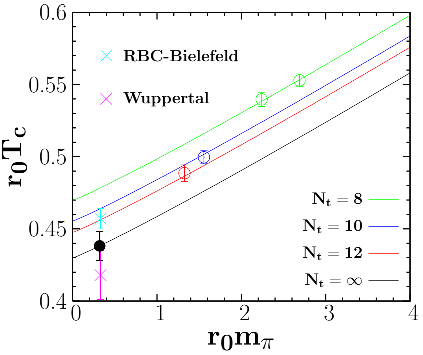

Fitting function

$$r_0 T_c(r_0 m_\pi, 1/N_\tau) = r_0 T_c(0,0) + C_{N_\tau} \frac{1}{N_\tau^2} + C_m (r_0 m_\pi)^d \qquad (1)$$

with $d = 1.08$

or alternatively

$$r_0 T_c(r_0 m_\pi, a/r_0) = r_0 T_c(0,0) + C_a \left(\frac{a}{r_0}\right)^2 + C_m (r_0 m_\pi)^d \qquad (2)$$

Result of fit acc. to (1)

$$r_0 T_c(r_0 m_\pi^{phys}, 0) = 0.438(6)(-7)(+13) \qquad (3)$$

Critical temperature

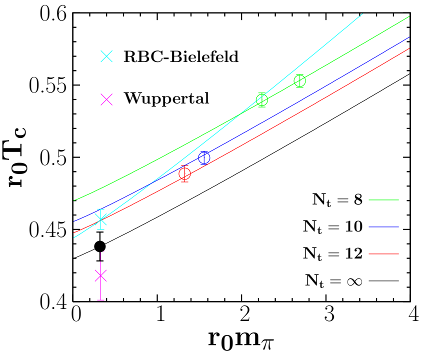

The string tensions around T_c

temperature range: $0.8 < T/T_c < 1.3$

spatial static potential: $r = R\ a$

$$a\ V_s(r) = \lim_{Z\to\infty} \log \frac{W(R,Z)}{W(R,Z+1)}$$

fitting ansatz:

$$V_s(r) = V_0 - \frac{\alpha}{r} + \sigma_s\ r$$

The string tensions around T_c

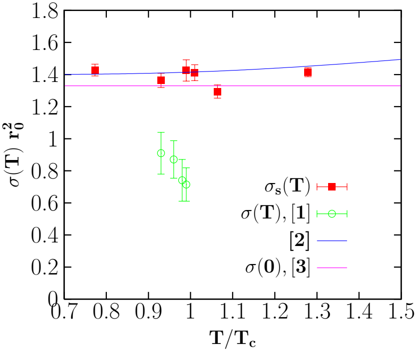

Distribution of the eigenmodes on the $Q = 0$ subsamples

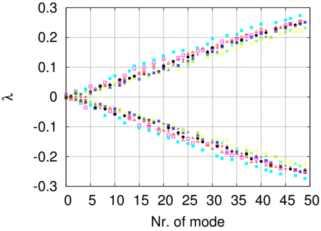

$\kappa = 0.1348$

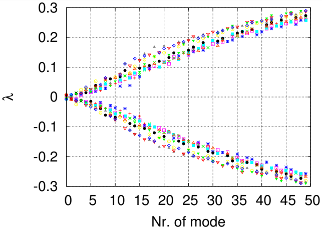

$\kappa = 0.1352$

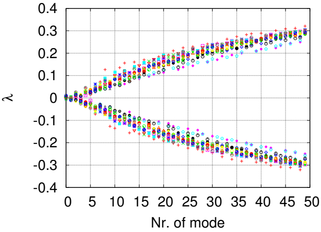

$\kappa = 0.1353$

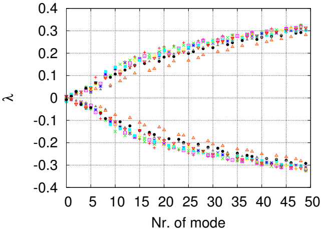

$\kappa = 0.1354$

Distribution of the eigenmodes on the $Q = 0$ subsamples

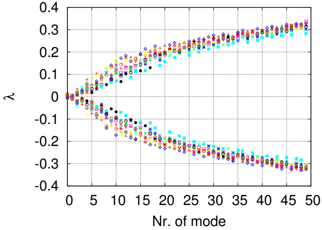

$\kappa = 0.1355$

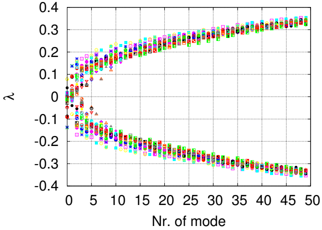

$\kappa = 0.1358$

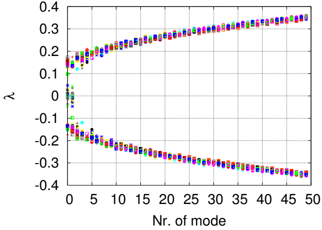

$\kappa = 0.1360$

The spectral density

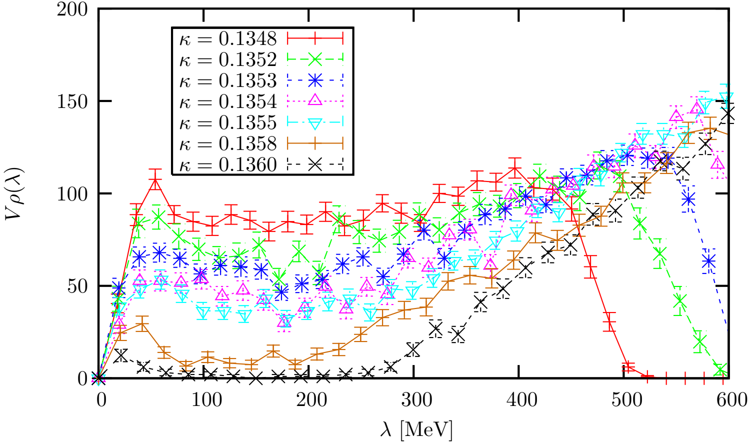

$\rho(\lambda) = \frac{1}{V}\left\langle \sum_{\bar\lambda} \delta(\lambda - \bar\lambda)\right\rangle$ taken over (nonzero) eigenmodes $\pm i\bar\lambda$ of $D^{\mathrm{imp}}(0)$.

Chiral susceptibility and Polyakov loop susceptibility

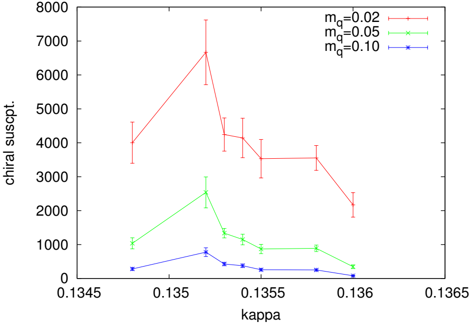

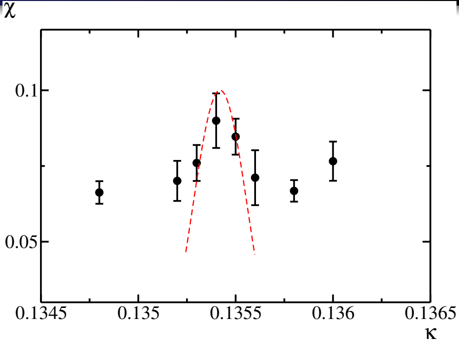

Chiral susceptibility

$$\chi_q \propto < (\mathrm{Tr}\, D^{-1}(m_q))^2 > - < \mathrm{Tr}\, D^{-1}(m_q) >^2$$

$$\langle \bar{\Psi}\Psi \rangle = \mathrm{Tr}\, D^{-1}(m_q) \approx \sum_\lambda 1/(i\lambda + m_q)$$

Polyakov loop susceptibility

$$\chi_L = N_s^3(< L^2 > - < L >^2)$$

$$L(\underline{s}) = \frac{1}{3}\, \mathrm{Tr} \prod_{s_4=1}^{N_t} U(\underline{s}, s_4)$$

Localisation of eigenmodes

Inverse **P**articipation **R**atio (IPR)

$$I = V \sum_x \rho(x)^2$$

with the scalar density

$$\rho(x) = {\Psi^{\lambda}}^{\dagger}(x)\Psi^{\lambda}(x)$$

using normalised eigenfunctions $\sum_x \rho(x) = 1$.

(Gattringer et al. 2001, Aubin et al. 2004, Gubarev et al. 2005, ...)

Characteristic features:

$I = V$	localised	$\rho(x) = \delta_{x,x'}$	support only on one lattice point x'
$I = 1$	nonlocalised	$\rho(x) = \frac{1}{V}$	maximally spread on all sites

Localisation of eigenmodes

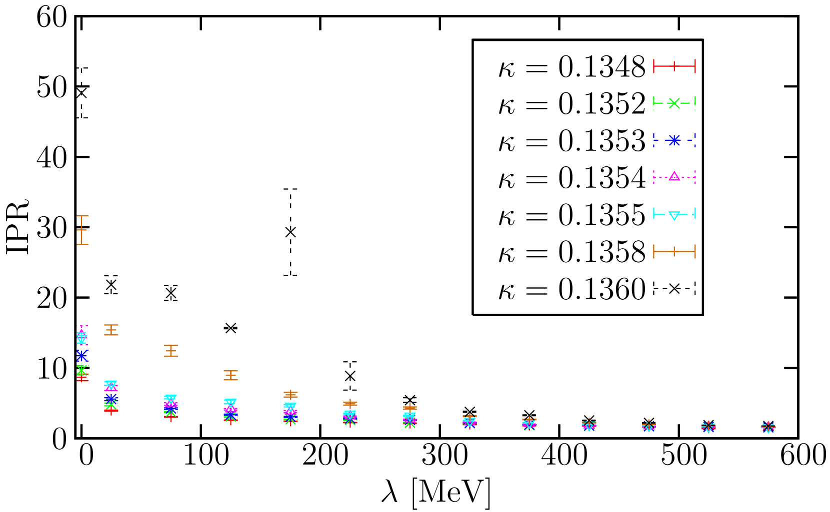

Local chirality of eigenmodes

Local chirality variable $X(x)$ (Horvath et al., 2001)

$$X(x) = \frac{4}{\pi} \arctan\left(\sqrt{\frac{\rho_+(x)}{\rho_-(x)}}\right) - 1 = \begin{cases} -1 & \textit{anti} - \textit{instanton} \\ +1 & \textit{instanton} \end{cases}$$

with the densities

$$\rho_\pm(x) = {\Psi^\lambda}^\dagger(x) P_\pm \Psi^\lambda(x)$$

and the projectors

$$P_\pm = \frac{1}{2}(1 \pm \gamma_5)$$

In the dilute instanton picture $X(x)$ should cluster in the confined phase near ± 1 for the low modes when one selects lattice points near the peaks of the scalar density.

Histograms of $X(x)$ averaged over the $Q = 0$ subsamples

1 % of the lattice sites with largest scalar density considered.

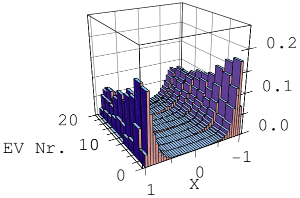

$\kappa = 0.1348$

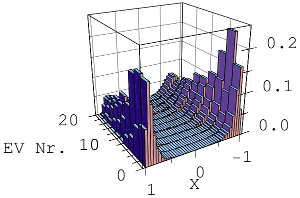

$\kappa = 0.1352$

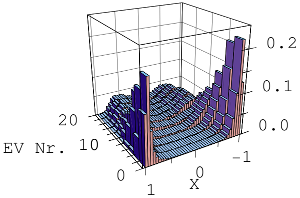

$\kappa = 0.1354$

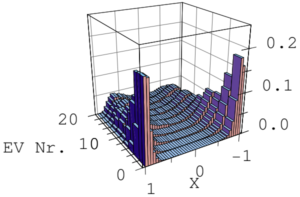

$\kappa = 0.1355$

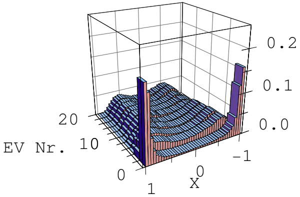

$\kappa = 0.1358$

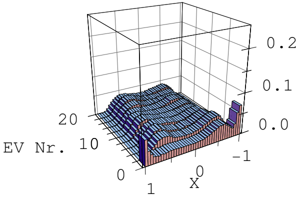

$\kappa = 0.1360$

Fermionic vs. gluonic def. of the topological charge

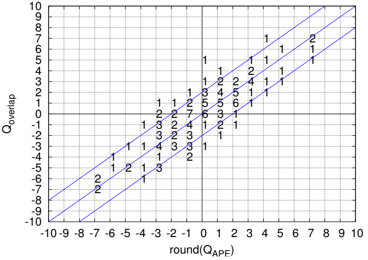

$\kappa = 0.1353$

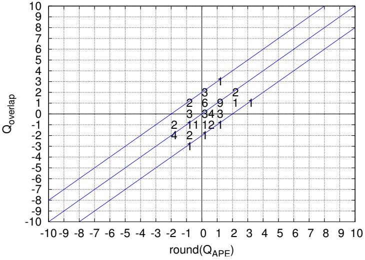

$\kappa = 0.1360$

Fermionic $\quad Q = \sum_{zeromodes} \langle \Psi_n | \gamma_5 | \Psi_n \rangle$, $\langle \Psi_n | \gamma_5 | \Psi_n \rangle = \pm 1$ for zeromodes

Gluonic $\quad$ 50 APE-smearing steps, improved clover definition (CP-PACS, PRD 64:114501)

$$Q_{\rm imp} = \sum_x \left\{ \frac{5}{3} Q_L^P(x) - \frac{2}{12} Q_L^R(x) \right\}, \; Q_L^X(x) = \frac{1}{32\pi^2} \epsilon_{\mu\nu\rho\sigma} \, {\rm Tr} \left(C_{\mu\nu}^X(x) C_{\rho\sigma}^X(x) \right).$$

$C_{\mu\nu}^P = \frac{1}{4} \, {\rm Im} \Big($  $\Big)$ and $C_{\mu\nu}^R = \frac{1}{8} \, {\rm Im} \Big($ 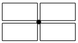 $+$ 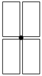 $\Big)$

Distribution of the topological charge Q

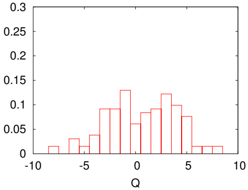

$\kappa = 0.1348$

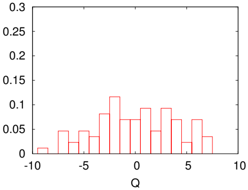

$\kappa = 0.1352$

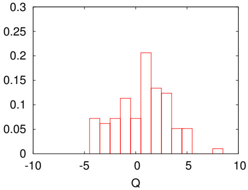

$\kappa = 0.1354$

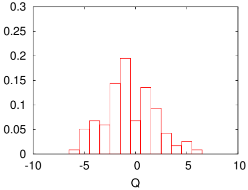

$\kappa = 0.1355$

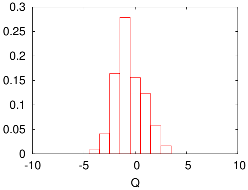

$\kappa = 0.1358$

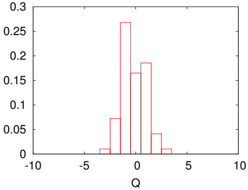

$\kappa = 0.1360$

The topological susceptibility

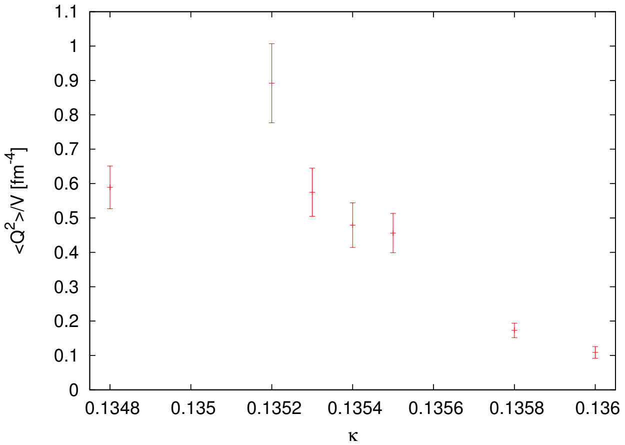

Local structure of the topological charge density $(16^3 \times 8)$

Topological charge density

$$q(x) = \frac{1}{2} \mathrm{Tr}\, \gamma_5 D(x,x), \quad Q = \sum_x q(x)$$

$C_q(r) = \langle q(0) q(r) \rangle \leq 0$ $(r > 0)$, but $\chi_t = \int dr\; C_q(r) > 0$

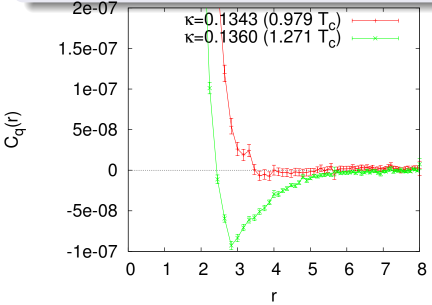

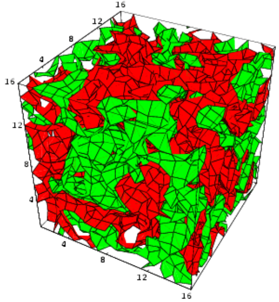

A measure for (anti-)selfduality (Gattringer, 2002)

Measure $R(x)$ for (anti-)selfduality

$$R(x) = 4/\pi \arctan r(x) - 1 = \begin{cases} -1 & \text{f. } F_{\mu\nu}(x) = +\widetilde{F_{\mu\nu}}(x) \\ +1 & \text{f. } F_{\mu\nu}(x) = -\widetilde{F_{\mu\nu}}(x) \end{cases}$$

$$r(x) = (\tilde{s}(x) - \tilde{q}(x))/(\tilde{s}(x) + \tilde{q}(x)) \, ,$$

action density: $\tilde{s}(x) = \mathrm{Tr}\, F_{\mu\nu}(x) F_{\mu\nu}(x) = \sum_{i,j=1}^{N} \frac{\lambda_i^2 \lambda_j^2}{2} f^a_{\mu\nu}(x)_{x,i} f^a_{\mu\nu}(x)_{x,j}$

charge density: $\tilde{q}(x) = \mathrm{Tr}\, F_{\mu\nu}(x) \widetilde{F_{\mu\nu}(x)} = \sum_{i,j=1}^{N} \frac{\lambda_i^2 \lambda_j^2}{2} f^a_{\mu\nu}(x)_{x,i} \widetilde{f^a_{\mu\nu}(x)}_{x,j}$

$$f^a_{\mu\nu}(x)_{y,j} = -\frac{i}{2} \;{}_y\langle j | \gamma_\mu \gamma_\nu T_a | j \rangle_x$$

Histograms of $R(x)$ averaged over the $Q = 0$ subsamples

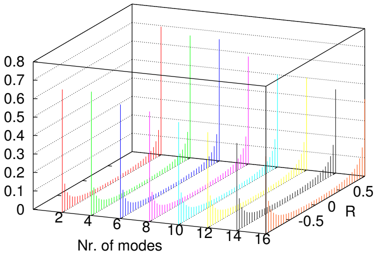

$\kappa = 0.1352$

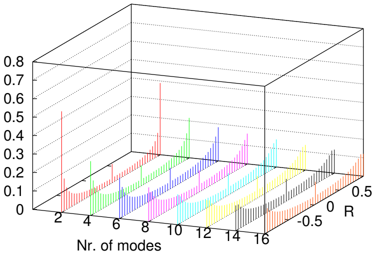

$\kappa = 0.1360$

Isosurfaces of $R(x)$: $R_{cut} = 0.97$

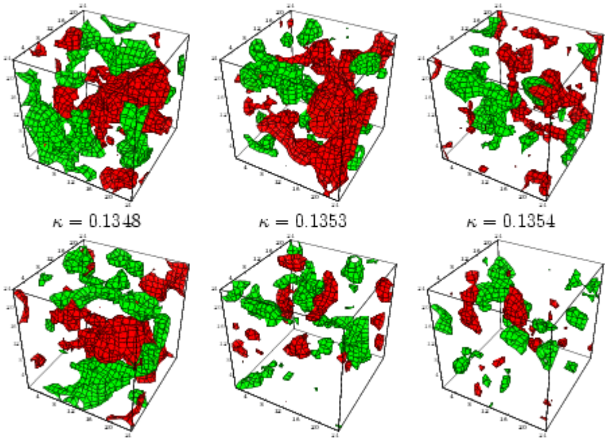

$\kappa = 0.1348$ $\kappa = 0.1353$ $\kappa = 0.1354$

$\kappa = 0.1355$ $\kappa = 0.1358$ $\kappa = 0.1360$

Cluster analysis of $R(x)$

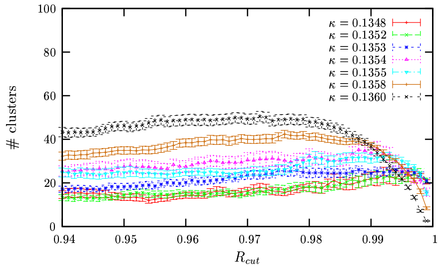

Number of R-clusters

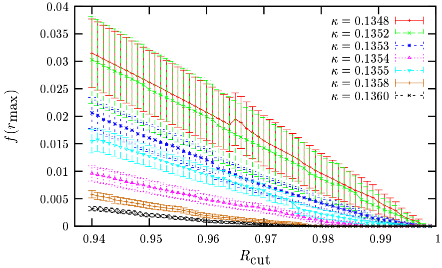

Connectivity of the clusters

(percolation iff $f(r_{\max}) > 0$)

Summary I

- The zero-modes and low-lying modes in the confined phase are strongly localised, while the higher modes are delocalised in both phases. The transition is preceded by the lowest modes becoming more localised before a gap opens.
- At low-T the low-lying modes show a strong signal of local chirality, which completely vanishes at high-T outside the spectral gap.
- Similar changes happen with the distribution of $R(x)$. In the high-T phase the clusters become less ,,classical" and the apparent (anti-) selfdual dominance is lost.
- Even for the largest investigated κ values at high-T some eigenvalues fall in the gap, which are extremely localised and still show a sign of local chirality.
- From the index we find a rapid drop of the top. susceptibility in the vicinity of the phase transition.
- The top. charge correlator changes at the phase transition, revealing a kind of short range charge compensation.

Summary I

- The zero-modes and low-lying modes in the confined phase are strongly localised, while the higher modes are delocalised in both phases. The transition is preceded by the lowest modes becoming more localised before a gap opens.
- At low-T the low-lying modes show a strong signal of local chirality, which completely vanishes at high-T outside the spectral gap.
- Similar changes happen with the distribution of $R(x)$. In the high-T phase the clusters become less ,,classical" and the apparent (anti-) selfdual dominance is lost.
- Even for the largest investigated κ values at high-T some eigenvalues fall in the gap, which are extremely localised and still show a sign of local chirality.
- From the index we find a rapid drop of the top. susceptibility in the vicinity of the phase transition.
- The top. charge correlator changes at the phase transition, revealing a kind of short range charge compensation.

Summary I

- The zero-modes and low-lying modes in the confined phase are strongly localised, while the higher modes are delocalised in both phases. The transition is preceded by the lowest modes becoming more localised before a gap opens.
- At low-T the low-lying modes show a strong signal of local chirality, which completely vanishes at high-T outside the spectral gap.
- Similar changes happen with the distribution of $R(x)$. In the high-T phase the clusters become less ,,classical" and the apparent (anti-) selfdual dominance is lost.
- Even for the largest investigated κ values at high-T some eigenvalues fall in the gap, which are extremely localised and still show a sign of local chirality.
- From the index we find a rapid drop of the top. susceptibility in the vicinity of the phase transition.
- The top. charge correlator changes at the phase transition, revealing a kind of short range charge compensation.

Summary I

- The zero-modes and low-lying modes in the confined phase are strongly localised, while the higher modes are delocalised in both phases. The transition is preceded by the lowest modes becoming more localised before a gap opens.
- At low-T the low-lying modes show a strong signal of local chirality, which completely vanishes at high-T outside the spectral gap.
- Similar changes happen with the distribution of $R(x)$. In the high-T phase the clusters become less ,,classical" and the apparent (anti-) selfdual dominance is lost.
- Even for the largest investigated κ values at high-T some eigenvalues fall in the gap, which are extremely localised and still show a sign of local chirality.
- From the index we find a rapid drop of the top. susceptibility in the vicinity of the phase transition.
- The top. charge correlator changes at the phase transition, revealing a kind of short range charge compensation.

Summary I

- The zero-modes and low-lying modes in the confined phase are strongly localised, while the higher modes are delocalised in both phases. The transition is preceded by the lowest modes becoming more localised before a gap opens.
- At low-T the low-lying modes show a strong signal of local chirality, which completely vanishes at high-T outside the spectral gap.
- Similar changes happen with the distribution of $R(x)$. In the high-T phase the clusters become less „classical“ and the apparent (anti-) selfdual dominance is lost.
- Even for the largest investigated κ values at high-T some eigenvalues fall in the gap, which are extremely localised and still show a sign of local chirality.
- From the index we find a rapid drop of the top. susceptibility in the vicinity of the phase transition.
- The top. charge correlator changes at the phase transition, revealing a kind of short range charge compensation.

Summary I

- The zero-modes and low-lying modes in the confined phase are strongly localised, while the higher modes are delocalised in both phases. The transition is preceded by the lowest modes becoming more localised before a gap opens.
- At low-T the low-lying modes show a strong signal of local chirality, which completely vanishes at high-T outside the spectral gap.
- Similar changes happen with the distribution of $R(x)$. In the high-T phase the clusters become less „classical“ and the apparent (anti-) selfdual dominance is lost.
- Even for the largest investigated κ values at high-T some eigenvalues fall in the gap, which are extremely localised and still show a sign of local chirality.
- From the index we find a rapid drop of the top. susceptibility in the vicinity of the phase transition.
- The top. charge correlator changes at the phase transition, revealing a kind of short range charge compensation.

Summary II

Different observables seem to deliver different κ_c values
($\rightarrow$ crossover nature of the phase transition ???):

- The chiral susceptibility shows a peak at $\kappa \approx 0.1352$ $< \kappa_c = 0.13542(6)$ as determined via the Polyakov loop susceptibility.
- A gap in the eigenmode spectrum does not open below $\kappa \approx 0.1358$.
- Above $R_{cut} \approx 0.97$ approx. (anti-)selfdual domains percolate through the spacial volume only for $\kappa < 0.1358$.